BBA - Molecular Basis of Disease xxx (xxxx) xxxx

Contents lists available at ScienceDirect

BBA - Molecular Basis of Disease

journal homepage: www.elsevier.com/locate/bbadis

Fasting reveals largely intact systemic lipid mobilization mechanisms in respiratory chain complex III deficient mice

Nikica Tomašić[a,b,c], Heike Kotarsky[d], Rejane de Oliveira Figueiredo[e], Eva Hansson[a], Matthias Mörgelin[f], Ivan Tomašić[g], Jukka Kallijärvi[e,h], Eskil Elmér[i], Matti Jauhiainen[j], Erik A. Eklund[a], Vineta Fellman[a,e,k,*]

[a] Lund University, Department of Clinical Sciences, Lund, Pediatrics, Lund, Sweden
[b] Karolinska University Hospital, Department of Neonatology, Stockholm, Sweden
[c] Faculty of Science, Department of Biology, University of Zagreb, Croatia
[d] Department of Pathology, Region Skåne, Lund University, Sweden
[e] Folkhälsan Research Center, Helsinki, Finland
[f] Lund University, Department of Clinical Sciences, Lund, Lund, Sweden
[g] Mälardalen University, Division of Intelligent Future Technologies, Västerås, Sweden
[h] Stem Cells and Metabolism Research Program, Faculty of Medicine, University of Helsinki, Helsinki, Finland
[i] Department of Clinical Sciences, Lund, Mitochondrial Medicine, Lund University, Lund, Sweden
[j] Minerva Foundation Institute for Medical Research, Biomedicum 2U, National Institute for Health and Welfare, Helsinki, Finland
[k] Children's Hospital, University of Helsinki, Helsinki. Finland

ARTICLE INFO

Keywords:
Mitochondrial disorder
Liver disease
OXPHOS
BCS1L
Fasting
Lipid metabolism

ABSTRACT

Mice homozygous for the human GRACILE syndrome mutation (*Bcs1l*$^{c.A232G}$) display decreased respiratory chain complex III activity, liver dysfunction, hypoglycemia, rapid loss of white adipose tissue and early death. To assess the underlying mechanism of the lipodystrophy in homozygous mice (*Bcs1l*$^{p.S78G}$), these and wild-type control mice were subjected to a short 4-hour fast. The homozygotes had low baseline blood glucose values, but a similar decrease in response to fasting as in wild-type mice, resulting in hypoglycemia in the majority. Despite the already depleted glycogen and increased triacylglycerol content in the mutant livers, the mice responded to fasting by further depletion and increase, respectively. Increased plasma free fatty acids (FAs) upon fasting suggested normal capacity for mobilization of lipids from white adipose tissue into circulation. Strikingly, however, serum glycerol concentration was not increased concomitantly with free FAs, suggesting its rapid uptake into the liver and utilization for fuel or gluconeogenesis in the mutants. The mutant hepatocyte mitochondria were capable of responding to fasting by appropriate morphological changes, as analyzed by electron microscopy, and by increasing respiration. Mutants showed increased hepatic gene expression of major metabolic controllers typically associated with fasting response (*Ppargc1a*, *Fgf21*, *Cd36*) already in the fed state, suggesting a chronic starvation-like metabolic condition. Despite this, the mutant mice responded largely normally to fasting by increasing hepatic respiration and switching to FA utilization, indicating that the mechanisms driving these adaptations are not compromised by the CIII dysfunction.

Summary statement: Bcs1l mutant mice with severe CIII deficiency, energy deprivation and post-weaning lipolysis respond to fasting similarly to wild-type mice, suggesting largely normal systemic lipid mobilization and utilization mechanisms.

Abbreviations: CIII, mitochondrial complex III; FA, fatty acid; RC, respiratory chain; HL, hepatic lipase activities; MEM, linear mixed-effect model; LPL, lipoprotein lipase activity; OXPHOS, oxidative phosphorylation; PHP, post-heparin plasma; PLTP, phospholipid transfer protein; PON-1, paraoxonase-1; TCA, tricarboxylic acid; WT, wild-type

* Corresponding author at: Lund University, Department of Clinical Sciences, Lund, Pediatrics, Klinikgatan 12, 221 84 Lund, Sweden.
E-mail addresses: nikica.tomasic@med.lu.se (N. Tomašić), rejane.figueiredo@helsinki.fi (R. de Oliveira Figueiredo), eva.hansson@med.lu.se (E. Hansson), matthias@colzyx.com (M. Mörgelin), ivan.tomasic@mdh.se (I. Tomašić), jukka.kallijarvi@helsinki.fi (J. Kallijärvi), eskil.elmer@med.lu.se (E. Elmér), matti.jauhiainen@thl.fi (M. Jauhiainen), erik.eklund@med.lu.se (E.A. Eklund), vineta.fellman@med.lu.se (V. Fellman).

https://doi.org/10.1016/j.bbadis.2019.165573
Received 3 June 2019; Received in revised form 30 September 2019; Accepted 1 October 2019

1. Introduction

Mitochondrial hepatopathies in newborn infants are rare and if subtle might be undiagnosed [1]. One of the several etiologies is respiratory chain (RC) complex III (CIII, ubiquinol-cytochrome *c* reductase) dysfunction caused by mutations in the nuclear gene *BCS1L* [2]. This gene encodes a protein (BCS1L), which is located in the inner mitochondrial membrane and functions as a translocase facilitating the assembly of Rieske iron-sulfur protein (RISP) into the pre-complex of CIII resulting in a catalytically active complex [3,4]. More than twenty mutations have been published causing a broad spectrum of clinical phenotypes [3]. The most severe phenotype is GRACILE syndrome (Fellman disease, OMIM 603358) caused by a homozygous point mutation (*c.A232G*, p.Ser78Gly) enriched in the Finnish population [5,6]. The acronym depicts the characteristic clinical findings: fetal Growth Restriction, Aminoaciduria due to proximal tubulopathy, Cholestasis, Iron accumulation, Lactic acidosis and Early death [5]. Motivated by the robust genotype-phenotype consistency [5,7], the Fellman group produced a knock-in mouse model carrying this mutation (*Bcs1l*$^{c.A232G}$) [8], the first viable disease model of CIII dysfunction. The homozygous mutant mice (*Bcs1l*$^{p.S78G}$) are healthy until weaning, after which they present with decreasing CIII activity, growth restriction, metabolic liver dysfunction, renal tubulopathy, and a short life span [8,9], thus phenocopying the human disorder [5,10]. CIII activity is not completely abolished in organs investigated in the mutant mice, but decreased to below 50% of controls in affected tissues (20%, 40%, 40% in liver, hearth and kidney respectively) [8]. The rapid disease progression to lethality at about one month of age in the C57BL/6JBomTac genetic background [9,11] is likely due to the inability to maintain blood glucose, resulting in lethal hypoglycemia.

The liver plays a central role in metabolism and ensures blood glucose and lipid homeostasis to meet the fuel requirements of other organs. In hepatocytes, two reciprocal pathways, glycolysis and gluconeogenesis, are responsible for glucose homeostasis. The main regulators of these opposing processes are hormones (insulin, glucagon and cortisol), and intracellular metabolites such as ATP and acetyl-CoA that is produced from β-oxidation. ATP and acetyl-CoA stimulate the anabolic direction with acetyl-CoA being an activator of gluconeogenesis [12]. During sudden food deprivation, hepatocytes release glucose mainly by glycogenolysis, but also through gluconeogenesis [13]. Fatty acid (FA) oxidation is considered critical during fasting for providing ATP and NADH to facilitate hepatic gluconeogenesis, and acetyl-CoA for ketogenesis if fasting progresses to prolonged starvation [14]. The capacity of the liver to respond to rapid changes in nutrient availability is dependent on a highly dynamic transcriptional regulatory network, particularly peroxisome proliferator-activated receptor alfa (PPARα). SIRT1, a nuclear NAD^+-dependent protein deacetylase is an important regulator of lipid homeostasis, especially FA oxidation. Increasing NAD^+ levels activate the sirtuins and have a positive effect on metabolism in different model organisms [15,16]. SIRT1 can either repress or activate the transcriptional activities of its target proteins (to which NF-kB and PGC-1α belong), and thereby regulate metabolic and stress pathways [17].

Crosstalk between liver and other organs, such as adipose tissue, is fundamental for metabolic homeostasis. In response to fasting, adipose tissue launches lipolysis leading to release of free FAs and glycerol into circulation. These are taken up by the hepatocytes, in which FAs are used for β-oxidation and/or triacylglycerol synthesis and their storage in lipid droplets, and glycerol in the gluconeogenetic pathway converted to glucose [18]. In skeletal muscles, glycogen and protein breakdown takes place, thereby providing alanine and lactate for gluconeogenesis in the liver [13]. Lactate is metabolized to pyruvate, a tricarboxylic acid (TCA) cycle substrate, but also used for gluconeogenesis in hepatocytes, which then release glucose for use in the muscle, a feed-back system named Cori cycle [19].

In mitochondria, ATP is generated through oxidative phosphorylation (OXPHOS), as the energy of reducing equivalents is converted into a proton gradient driving the ATP synthase. Reducing equivalents are supplied from the cytoplasmic glycolytic pathway, from processes in the mitochondrial matrix (TCA cycle and β-oxidation). A dysfunction in CIII not only results in energy deprivation due to decreased electron flow in RC but may also compromise supercomplex (respirasome) formation [11] as CIII has a central role in their formation together with complex I and complex IV [20]. Respirasomes are located in the planar part of cristae and have been suggested to enhance electron flow and channeling of substrates [21,22].

Almost complete loss of white adipose tissue is a dramatic manifestation in both GRACILE syndrome patients and *Bcs1l*$^{p.S78G}$ mice [5,8]. Concomitantly, the patients show hepatic steatosis and the mice microvesicular fat accumulation in hepatocytes. Fat accumulation is not seen in other tissues than liver, which suggests that it results from normal mobilization of lipids from white adipose tissue to liver for fuel. However, the basic lipid mobilization and transport in these mice have never been investigated. Therefore, we subjected *Bcs1l*$^{p.S78G}$ mice at age 25–28 days (P25–28) to a short fast and measured hepatic and plasma lipids and parameters of energy metabolism.

2. Materials and methods

2.1. Animals

The *Bcs1l*$^{c.A232G}$ mouse strain, > 99% congenic in C57BL/6JBomTac background [9,11], was maintained on a rodent diet (Labfor R34, Lantmännen, Stockholm, Sweden) in a vivarium with 12 h light/dark cycles at 22 °C and water ad libitum [8]. Homozygous (*Bcs1l*$^{p.S78G}$) and littermate controls, either wild-type (WT) or heterozygous mice that are phenotypically identical to WT, were weaned at postnatal day 19–21 (P19–21). Their health and weight were followed daily, as previously described [9]. When the homozygotes showed signs of disease either as weight reduction or behavioral changes (at P25–28), but well before end-stage disease, they were randomized to a 4-hour fast or normally fed period between 2 and 6 pm. Pair-matched WT animals from the same or the next litter underwent the same procedure. In total 61 animals (Table S1) were included in the four groups; fasted or fed homozygotes (15 and 14, respectively) and WT (15 and 17, respectively). The weight of mutant mice was lower (mean ± SD in females 8.1 ± 0.9 g and males 9.7 ± 1.1 g) than that of WT mice (females 12.6 ± 1.6 g and males 15 ± 1.7 g). At least 5 animals per group were used for the assessments (histology, plasma insulin, respirometry, gene expression, lipid studies and electron microscopy). Additional 17 normally fed animals (7 homozygotes and 10 WT, P27–28) were included for blood sampling with cardiac puncture for paraoxonase-1 (PON-1) analysis. To assess lipase activities, additional 12 normally fed mice (6 homozygotes, 6 WT, age P27) were used to assess lipase activities from post-heparin plasma samples obtained with cardiac puncture 15 min after intraperitoneal injection of 0.1 IU heparin per g body weight. Total number of animals used was 90.

Before and after fasting, a tail blood sample was obtained during transient anesthesia with isoflurane (Forene, AbbVie AB, Solna, Sweden). The animals were sacrificed using cervical dislocation after the second tail blood sampling, the weight was measured, and a third blood sample was obtained by immediate heart puncture. Liver tissue was collected directly thereafter. Plasma or serum samples were prepared and frozen at −80 °C until further use. Liver tissue samples were processed according to 4 specific protocols; 1) snap frozen at −80 °C, 2) fixed in 4% buffered formalin, 3) collected in EM fixation buffer or 4) soaked in ice cold isolation buffer for mitochondrial isolation.

2.2. Ethics statement

Animal experiments were performed with the approval of the Lund regional animal research committee, Sweden (permits, M245-11,

M337-12, 31-8265/08) according to national regulations and ARRIVE recommendations. All efforts were taken to ameliorate suffering.

2.3. Measurements of ketone bodies, glucose and lactate in whole blood

Blood chemistry was measured from tail blood using test strips: glucose with FreeStyle Freedom (Abbott Diabetes Care Inc., Alameda, CA, USA), ketone bodies with Precision Xceed (Abbott Diabetes Care Inc., Alameda, CA, USA) and lactate with Lactate Pro (ARKRAY Inc., Kyoto, Japan).

2.4. Insulin measurement and HOMA-IR index calculation

Plasma insulin concentrations were analyzed in duplicates using Ultra Sensitive Mouse Insulin ELISA Kit (Crystal Chem #90080) with low-range assay mode (according to the manufacturer's instructions) using plasma samples obtained by cardiac puncture. Absorbance values were measured with the Varioskan Flash Multimode Reader (Thermo Scientific) and analyzed using the accompanying software. The homeostasis model assessment for insulin resistance (HOMA-IR) was calculated as the product of the fasting blood glucose value (measured in mmol/l) and the fasting plasma insulin value (measure in mU/l) divided by 22.5 [23].

2.5. Histology

Formalin-fixed liver samples were processed according to standard pathology laboratory routine and paraffin embedded. Sections were stained with hematoxylin and eosin (H&E) for morphology and periodic acid–Schiff (PAS) with and without diastase for glycogen. Standard Oil-Red-O (ORO) staining for triglycerides was performed on snap frozen liver tissue sections.

2.6. Isolation of mouse liver mitochondria

Liver tissue, collected in isolation buffer (320 mM Sucrose, 10 mM Tris, 2 mM EGTA, pH 7.4 on ice), was homogenized in 2 ml of the buffer supplemented with 0.1% bovine serum albumin. Mitochondria were prepared from homogenates by sequential centrifugation including density purification on 19% Percoll (GE Healthcare, Amersham, UK) [24]. Mitochondrial protein concentrations were estimated by measuring 280 nm absorbance using a Nanodrop® spectrophotometer (Fisher Scientific, Gothenburg, Sweden).

2.7. Lipid analyses

Cellular lipids were extracted from snap-frozen liver samples by the Folch method [25] and triglycerides were measured as glycerol after chloroform–methanol extraction and hydrolysis. Briefly, liver tissue (50–100 mg) was mechanically homogenized and sonicated in 1 ml 95% methanol and mixed with 2 ml chloroform. The organic phase was washed twice with 0.9% NaCl solution and dried under nitrogen. The residuals were dissolved in 200 µl of tetraethylammoniumhydroxide (diluted 1:28 with 95% ethanol (v:v)) and incubated at +60 °C for 30 min in the presence of added 200 µl of 0.05 M HCl. The formed glycerol was measured enzymatically using a commercial triglyceride analysis kit (GPO-PAP 1488872, Roche Diagnostics, Mannheim, Germany).

Total cholesterol and choline-containing phospholipids (PC, lysoPC, SM) were measured from the solvent phase after initial chloroform–methanol extraction, using the commercial enzymatic assays (Cholesterol CHOD-PAP kit (Roche Diagnostics, Mannheim, Germany) and Phospholipids B kit (Wako Chemicals, Osaka, Japan)).

Plasma free FA concentrations were measured by an enzymatic colorimetric method (NEFA-HR(2), Wako Chemicals, Osaka, Japan). Plasma concentration of glycerol was determined by an enzymatic colorimetric assay (Free glycerol FS, DiaSys, Diagnostic Systems GmbH, Holzheim, Germany).

Plasma phospholipids (choline-containing phospholipids, i.e. phosphatidylcholine (PC), lysoPC and sphingomyelin) were analyzed using the Phospholipids B kit (Wako Chemicals, Osaka, Japan) or Pureauto S PL-kit (Daiichi Pure Chemicals, Tokyo, Japan); triglycerides using the Triglycerides GPO-PAP-kit (Roche Diagnostics, Mannheim, Germany); free cholesterol using the Wako Free Cholesterol C kit (Wako Chemicals, Osaka, Japan) and total cholesterol using the Cholesterol CHOD-PAP kit (Roche Diagnostics, Mannheim, Germany).

2.8. Plasma lipoprotein analyses

Mouse plasma apolipoprotein A-I (apoA-I) was quantified using a sandwich enzyme-linked immunosorbent assay (ELISA) as described [26].

Plasma lipoproteins were fractionated on Superose 6 HR 10/30 size-exclusion chromatography column (GE Healthcare, Buckinghamshire, UK) using fast-protein liquid chromatography system (FPLC; Merck-HPLC System) as described previously [27].

The column was operated at room temperature and was equilibrated with a 10 mM Na-phosphate/140 mM NaCl buffer, pH 7.4. Samples of 110–150 µl (mouse plasma) were applied on the column at a flow rate of 0.5 ml/min, and fractions (0.5 ml) were collected and analyzed for cholesterol, triglycerides, choline-containing phospholipids and apoA-I.

2.9. Measurements of lipid metabolism-related enzyme activities

Post-heparin plasma (PHP) lipoprotein and hepatic lipase activities (LPL and HL) were measured from normally fed mice to reveal a possible effect of the mutation using a previously described method [28]. Briefly, [Carboxyl-14C]-Triolein (S.A. 2.2 GBq/mmol, PerkinElmer) and glyceryl trioleate (Sigma-Aldrich, Darmstadt, Germany) emulsified in the presence of gum arabic was used as substrate. PHP samples were incubated in the presence of the substrate and human serum (as a source for apoC-II, LPL cofactor) for 1 h at +37 °C. The reaction was stopped by addition of 3.25 ml of methanol-chloroform-heptane (1.41:1.25:1.00, v/v/v) and 0.75 ml of 0.14 M potassium carbonate/borate buffer (H_2CO_3, 0.14 M, K_3BO_3, 0.14 M, pH 10.5). Hydrophilic phase (bovine serum albumin-FAs) and hydrophobic phase (triolein) were separated by centrifugation and radioactivity was measured from both fractions by liquid scintillation counting (Wallac LS Counter, Turku, Finland). To distinguish between HL and LPL activities, HL lipolytic activity was measured in the presence of 1 M NaCl, as this is known to inhibit LPL activity but not hepatic lipase activity. Values obtained using high salt were attributed to HL activity and LPL activity was calculated by subtracting the HL activity from the total PHP lipolytic activity. Lipolytic activity was expressed as µmol of free FAs released per hour per ml of PHP.

Phospholipid transfer protein (PLTP) activity (nmol/ml/h) was determined with a radiometric method as described [29]. The intra- and inter-assay coefficients of variability (CVs) for PLTP were 9% and 12%, respectively. Paraoxonase-1 (PON-1) activity was measured with a chromogenic method [30]. The intra-assay and inter-assay CVs for PON-1 measurements were 10% and 7%, respectively.

2.10. High resolution respirometry

Oxygen consumption of freshly isolated mitochondria (protein concentration 250 µg/ml) was measured using an Oroboros Oxygraph-2 k equipped with the DatLab 4 software (Oroboros Instruments, Innsbruck, Austria). Experiments were run at 37 °C in mitochondrial respiration medium MIR05 supplemented stepwise with substrates and inhibitors for individual complexes, using the SUIT protocol by sequential addition of complex I and complex II substrates, uncoupler, and inhibitors [8,31].

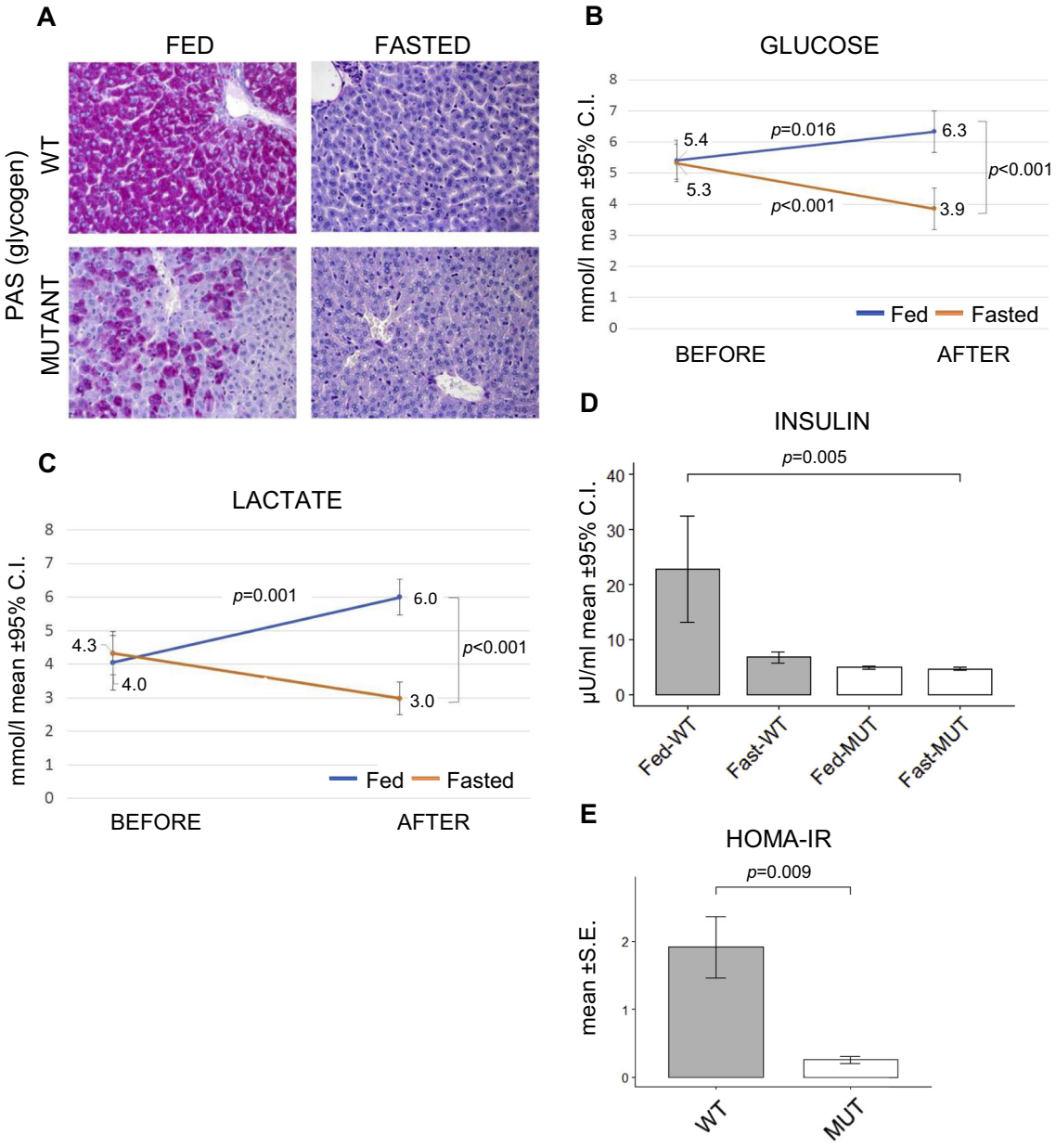

Fig. 1. Fasting-induced changes in carbohydrate metabolism in liver and blood in homozygous *Bcs1l* mutant (*Bcs1l*$^{p.S78G}$) mice and controls (WT). (A) PAS staining for glycogen. (B) Arterial blood glucose values before and after fasting (i.e. the occasion in the linear mixed-effect model, MEM). A blood glucose concentration below 3.4 mmol/l is considered hypoglycemia in mice. (C) Arterial blood lactate. Differences in values before and after fasting (B, C) are shown as differences in mean, together with effect of fasting obtained from MEM analyses. (D) Plasma insulin concentration and (E) HOMA-IR index.

2.11. Electron microscopy

Approximately 1 mm^3 pieces of liver tissue samples, obtained immediately after the animal was sacrificed, were fixed in 1.5% glutaraldehyde, 1.5% paraformaldehyde in 0.1 M Sörensen buffer pH 7.2. The fixed samples were thereafter prepared for ultrathin sectioning and subjected to transmission electron microscopy (TEM) according to standard methods. Specimens were examined in a Philips/FEI CM 100 BioTWIN transmission electron microscope at 60 kV voltage. Images were recorded with a side-mounted Olympus Veleta camera with a resolution of 2048 × 2048 pixels (2 k × 2 k).

Area, cristae number and thickness, and the shape of hepatocyte mitochondria were determined manually from images in Adobe Photoshop CS5. Cross sectional area was determined by manually selecting the longest and shortest axis of each mitochondrion. Approximately 100 different hepatocytes were chosen at random locations and layers throughout at least 10 different specimen preparations per animal. Around five mitochondria per hepatocyte, chosen at random, were measured, yielding approximately 500 investigated mitochondria per animal.

2.12. RNA isolation and quantitative PCR

RNA was extracted from snap frozen liver tissue using the RNeasy Mini kit and RNase free DNase set according to the manufacturer's recommendations (Qiagen GmbH, Düsseldorf, Germany), and RNA quantity and quality were analyzed with Nanodrop® spectrophotometer (Fisher Scientific, Gothenburg, Sweden) and agarose gel. For cDNA synthesis 500 ng total RNA were used with Taqman® reverse transcription reagents (Fisher Scientific, Gothenburg, Sweden) using random hexamer primers included in the kit. The resulting cDNA was used as template in real time reactions on a StepOne cycler (Thermo

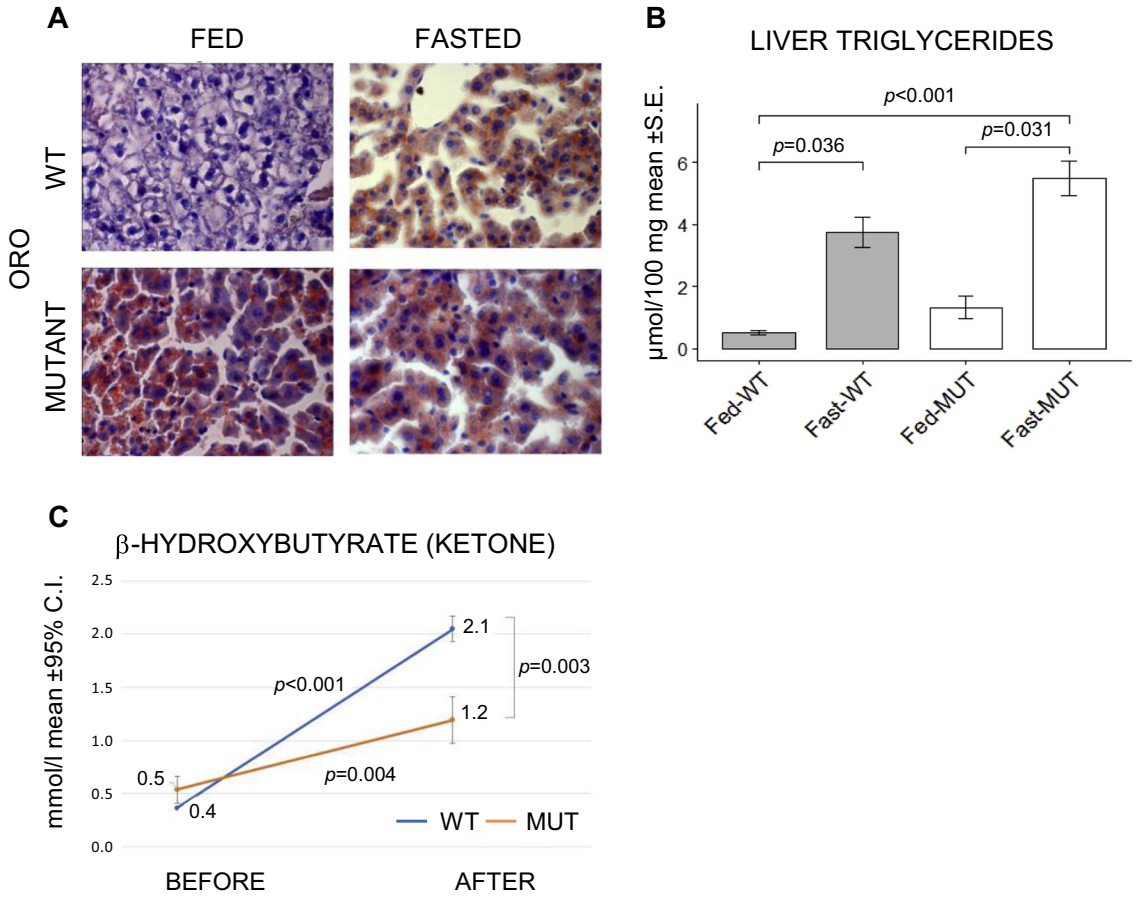

Fig. 2. Fasting-induced changes in lipid metabolism in liver and blood in *Bcs1l*$^{p.S78G}$ mice. (A) ORO staining for neutral lipids. (B) Concentration of triglycerides in liver tissue and (C) Blood ketone bodies. Differences in values before and after fasting are shown as differences in mean, together with effect of fasting obtained from MEM analysis.

Fisher Scientific) using Taqman Gene Expression assays (Thermo Fisher Scientific) as listed in Table S3. Expression values were normalized against *Gapdh* (Mm9999915_g1).

2.13. Statistical analysis

Linear mixed-effect models (MEMs) were used for the analysis of responses to fast with blood glucose, ketone and lactate as outcomes. The principal interests were to evaluate the effect of genotype (*GENOT*), fasting (*FAST*) and occasion (*OCC*, defined as the timepoint before or after fasting) on outcome variables and possible interaction between these variables. All models were adjusted for age, weight (*WG*) and litter size (*LITTSIZE*) describing the number of mice in the respective animal litter. Models were also adjusted for a random effect of litter and mouse. When there was significant interaction effect, multiple comparisons were carried out to check the differences, separately in categories of the variables evolved in interaction.

The general MEM used in this study may formally be described as follows:

$$OUT_{lmt} = \beta_1 * FAST_{lm} + \beta_2 * OCC_{lm} + \beta_3 * GENOT_{lm} + \beta_4 * AGE_{lm} + \beta_5 * WG_{lm} + +\beta_6 * LITTSIZE_l + \beta_7 (FAST_{lm} * OCC_{lm}) + \beta_{12} (GENOT_{lm} * FAST_{lm} * OCC_{lm}) + b_{0l} + b_{0lm} + \epsilon_{lmt},$$

where *OUT* is one of the outputs (GLUCOSE, ketone, lactate, L/G ratio) for litter *l*, mouse *m* and occasion *t* (before or after fasting or fed period, respectively). The estimated parameters of the model were the regression coefficients β_1, β_2, β_3, β_4, β_5, β_6 for each independent variable, β_7, β_{12} for the interactions terms, b_{01} and b_{0lm} for the random effects, and ε_{lmt} the error variance.

Group comparisons for all other variables in the study were analyzed using the Kruskal-Wallis test. All analyses were conducted using R-package version 3.5.1, except for the qPCR analysis where SPSS 22 was used to calculate Wilcoxon rank sum test. Mann-Whitney *U* test was used for electron microscopy analyses. A significance level of 5% was adopt for all tests.

3. Results

3.1. CIII deficient *Bcs1l*$^{p.S78G}$ mice respond to fasting by further hepatic glycogen depletion and hypoglycemia

In normally fed WT mice, hepatocytes contained abundant glycogen, and a 4-hour fast was sufficient to decrease the hepatic glycogen reserves (Fig. 1A). Fed homozygous mice (*Bcs1l*$^{p.S78G}$) showed glycogen depletion with scattered deposits remaining, as shown previously [8,9]. Fasted homozygotes had no detectable glycogen in the liver (Fig. 1A).

Blood glucose concentration was lower in the mutant mice compared to WT mice (Supplemental Table S2), independently of the occasion (meaning before and after the experiment) or if they were fasted ($p = 0.003$). There was a significant ($p < 0.001$) interaction between fasting and occasions; glucose concentration decreased by mean 1.5 mmol/l among fasting mice ($p < 0.001$) and increased by 0.9 mmol/l among fed mice ($p = 0.016$), regardless of the genotype (Fig. 1B). No interaction was found between genotype, fasting and occasions (genotype*fasting*occasions, $p = 0.849$). However, as the baseline was lower, fasting resulted in lower blood glucose concentrations in homozygous mutant carriers compared to WT mice

($p < 0.001$), leading to hypoglycemia (< 3.4 mmol/l) in twelve out of fourteen mutant animals, eight displaying values below 2.5 mmol/l indicating severe hypoglycemia.

Plasma insulin concentrations in both fed and fasted mutant mice were as low as in fasted WT (Fig. 1D). The HOMA-IR index was significantly lower in fasted mutant mice than in fasted WT, thus excluding insulin resistance (Fig. 1E).

Blood lactate concentration in the homozygotes was similar before (mean ± SD 4.19 ± 1.82 mmol/l) and after (3.32 ± 1.17 mmol/l) fasting and the lactate to glucose ratio was significantly higher than in WT mice, independently of fasting or occasion (Table S2). In fed animals the lactate was increased after the intervention irrespective of genotype (Fig. 1C).

3.2. Fasting results in normal hepatic fat accumulation and ketogenesis in *Bcs1l*$^{p.S78G}$ mice

Fasting increased hepatic neutral lipid content in WT mice, as shown by Oil-Red-O (ORO) staining (Fig. 2A). In homozygotes, the lipid accumulation was present already in the fed state, as previously shown [8,9] and increased upon fasting (Fig. 2A). We quantified these findings with tissue triglyceride measurements (Fig. 2B).

Both WT and mutant mice had a significant increase in blood ketone (β-hydroxybutyrate) concentration after fasting (Fig. 2C). However, on average the mutant mice had a significantly smaller increase in the circulating ketone bodies than the WT mice.

3.3. Fasting induces normal lipid mobilization in *Bcs1l*$^{p.S78G}$ mice

Fasting resulted in increased free FA concentration in plasma in both mutant and control mice (Fig. 3A). Glycerol, the other product of triglyceride hydrolysis in adipose tissue, was highly increased in plasma of WT mice by fasting. Surprisingly, plasma glycerol remained low in the *Bcs1l*$^{p.S78G}$ mice (Fig. 3B), despite similar increase in free FAs, suggesting rapid clearance from plasma.

Plasma concentrations of triglycerides, choline-containing phospholipids, cholesterol, and apolipoprotein A1 were similar in homozygous and WT mice, with no significant differences between fed and fasted groups (Fig. 3C–F). Activity of PLTP, a mediator of net transfer and exchange of phospholipids between different lipoproteins, was also similar in the four groups (Fig. 3H). We also assessed lipoprotein profiles in fasted and fed mutant and WT mice. No clear differences were found in the distribution of major lipoproteins, i.e. VLDL, LDL and HDL in mutant mice. In WT mice, however, fasting resulted in an increase of HDL levels (Fig. S1). Hepatic (HL) and lipoprotein lipase (LPL) activities were assessed in post-heparin plasma samples using radiometric method where free FA liberation from the substrate is quantified. No effect of the mutation was found on the lipase activities (Fig. 3G).

Activity of paraoxonase 1 (PON1), an enzyme that is synthesized in liver, bound to HDL particles in circulation and considered as an important circulating antioxidant, was significantly decreased in mutant animals (Fig. 3I).

3.4. Liver mitochondria of *Bcs1l*$^{p.S78G}$ mice can adjust respiration and ultrastructure in response to fasting despite severe CIII dysfunction

High-resolution respirometry (Fig. 4) of isolated liver mitochondria showed that complex I related phosphorylating states were similar in fed WT and mutant mice. Oligomycin induced (complex V inhibition) non-phosphorylating respiration rates (LEAK) were lower in mutant mice. Fasting had a general (apparent in practically all respiratory states) enhancing effect on respiration and this was most prominent in mutant mice and for non-phosphorylating respiration rates. To detect the CIII deficiency in the mutant mice in respirometry both complex I and II substrates were needed, as complex I-linked respiration is not necessarily affected [8,11].

Mitochondria are dynamic organelles that adapt their ultrastructure upon fasting [32]. Electron microscopy showed typical morphological changes (increased cross-sectional area, elongation, increased distance between cristae and crista thickness, number of cristae per mitochondrion) in WT mitochondria after 4 h of fasting (Fig. 5A). Fed mutant mice had more elongated mitochondria and less cristae than WT. In addition, mutants had less ribosomes and less endoplasmic reticulum (ER) compared to WT (Fig. 5B). Fasting in mutants resulted in additional elongation and swelling as shown by cross sectional area, increased cristae distance and thereby less cristae (Fig. 5C).

3.5. Hepatic gene expression reveals largely normal transcriptional response to fasting in *Bcs1l*$^{p.S78G}$ mice

Main metabolic controllers and downstream genes involved in metabolic switch upon fasting were analyzed using qPCR (Table S3). The 4-hour fast was enough for WT animals to switch on upregulation of the main metabolic controllers nicotinamide phosphoribosyltransferase (*Nampt*), PGC-1α (*Ppargc1a*), CREB Regulated Transcription Coactivator (*Crtc2*) and sirtuins (*Sirt1*, *Sirt3*). The effect was also clear on downstream key enzymes of the metabolic pathways: gluconeogenesis (*Pck1*), ketogenesis (*Hmgcl*), alanine metabolism (*Alat*) and β-oxidation (*Acox1*, *Cpt1a*). Fed mutant mice had a significant upregulation of *Ppargc1a* (6.4-fold increase compared to WT), *Crtc2*, *Sirt1* (2.3-fold), *Pparγ* (6.2-fold), *Fgf21* (6.5-fold), *Pck1*, *Cd36* (4.5-fold) and a significant decrease in FA synthase (*Fasn* 0.3 of WT). A further upregulation in response to fasting was only seen in *Ppargc1a* (2.5-fold), whereas *Fasn* was significantly downregulated (0.5 of fed mutant level). Additional upregulated genes in fasted mutants were the main energy and nutrient sensor 5′-AMP-activated protein kinase (*Prkag2*, 1.7-fold), beta-oxidation genes (*Acox1* 1.9-fold and *Cpt1a* 2-fold), alanine metabolism (*Alat* 2.1-fold), *Namt* (1.5-fold), and mitochondrial uncoupling protein 2 (*Ucp2*, 2.2-fold). However, there was no significant change in the gene expression of the key carbohydrate gluconeogenic enzyme (*Pck1*). *AldoB*, an enzyme operating in both directions was slightly upregulated (1.4-fold) in mutants in response to fasting, but the key ketogenic enzyme HMG-CoA lyase was not.

4. Discussion

In mitochondrial respiratory chain (RC) deficiencies, also referred to as OXPHOS disorders, ATP synthesis by oxidative phosphorylation is compromised. Subsequently, the deranged energy metabolism typically manifests in skeletal muscle, heart or central nervous system, but can also lead to liver disease with severe neonatal metabolic crisis, such as in CIII deficient GRACILE syndrome patients. Due to the defective oxidative energy metabolism, these patients and *Bcs1l*$^{p.S78G}$ mice carrying the patient mutation apparently utilize their hepatic glycogen reserves for glycolysis, resulting in glycogen depletion and fasting-like state [5,6,8–10]. The main aim of this study was to assess if the canonical response to nutrient deprivation, i.e. switch to glycogenolysis and then to fatty acid utilization, is intact in the CIII deficient mice *Bcs1l*$^{p.S78G}$ mice. For this investigation, we selected the age window P25–28, well before end-stage disease to avoid death due to hypoglycemia. The short 4-hour fast was sufficient to completely deplete liver glycogen and induce ketogenesis in both WT and mutant animals. In a study using different durations of fasting in P70 old mice, a 4-hour fast resulted in a similar increase in free FAs, glycerol and ketones as in our WT animals [33]. Therefore, we conclude that the 4-hour fast was sufficient for investigation of the physiological response to fasting but avoided adverse effects to the sick mice. For practical reasons the animals were fasted in afternoon, which might have resulted in a smaller effect than if fasted during night, when they are more active and need more energy.

Surprisingly, albeit the *Bcs1l* mutants are growth restricted with chronic starvation-like state [8,9], with significant upregulation of

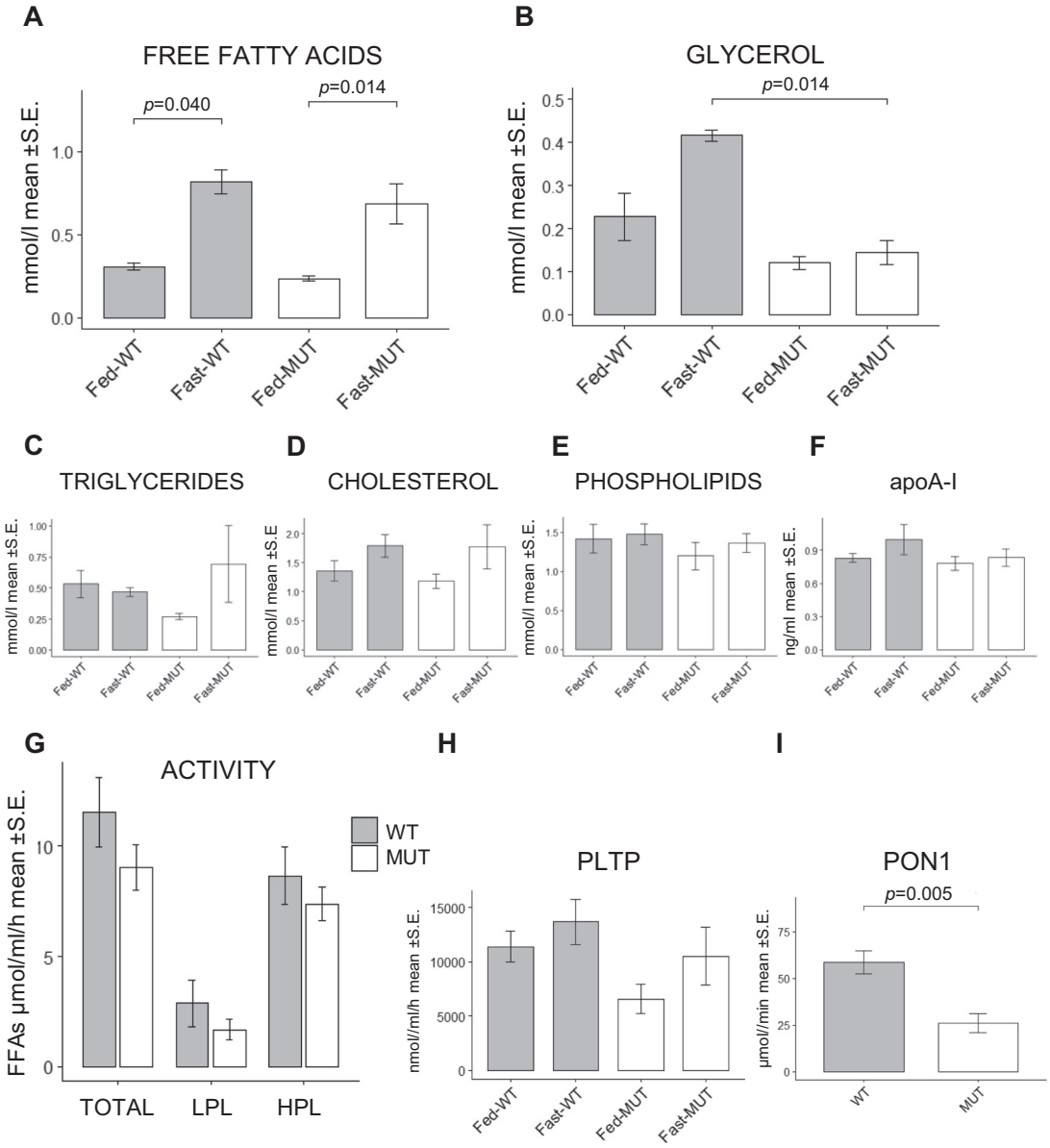

Fig. 3. Effect of fasting on plasma lipids, glycerol and lipase activities in *Bcs1l*$^{p.S78G}$ mice. Concentration of (A) plasma free fatty acids, (B) glycerol, (C) triglycerides, (D) cholesterol, (E) phospholipids and (F) apoA-I in fed and fasted mice. (G) Activities of lipoprotein lipases (LPL) and hepatic lipases (HPL) in post-heparin plasma. (H) Plasma phospholipid transfer protein (PLTP) activity and (I) serum PON-1 activity. Significant differences are indicated (p-values from Kruskal-Wallis test).

hepatic *Ppargc1a*, *Sirt1* and *Fgf21* expression [34], they were able to induce further lipolysis in response to fasting as shown by increased plasma free FAs. Since we observed no increase in LPL activity and low insulin levels, insulin being a master regulator of LPL [35], our data indicate that the free FAs were derived from normal route, i.e. TG-lipid droplet lipolysis in adipose tissue. In line with the increased liver lipid content, increased hepatic expression of the fatty acid receptor *Cd36* [36] suggested increased uptake of circulating FAs into hepatocytes. Concomitantly, hepatic fatty acid synthase (*Fasn*) expression was decreased, which is a well-known response to fasting [33,37]. Moreover, fasting-induced upregulation of the key genes involved in beta-oxidation and ketogenesis, *Acox1* and *Cpt1a*, in both mutant and WT animals suggested that the mutants could induce transcriptional response for utilization of circulating free FAs to compensate for glucose deficiency [38,39]. In our previous study, high-fat, low-carbohydrate ketogenic diet had a beneficial effect on liver histology and mitochondrial ultrastructure in *Bcs1l*$^{p.S78G}$ mice [40]. Although the mechanism of this improvement remained unclear, the study suggested that the mice could normally utilize fatty acid β-oxidation for energy production in the absence of glucose. In the current study, the strikingly low plasma glycerol in the mutants most probably resulted from a rapid uptake of glycerol into hepatocytes, in which glycerol is metabolized for gluconeogenesis and also provides reducing substrates for mitochondria [18]. This may have contributed to the improved total respiratory capacity we observed in fasted homozygotes. In our previous metabolomics study of liver tissue, dihydroxyacetonephosphate and 3-phospho-glyceraldehyde concentrations were decreased at all studied ages, P14, P24, and P30 [41] supporting that glycerol was used for gluconeogenesis.

PPARα is a master transcriptional regulator of liver intermediary metabolism and is needed in newborn mice for ketogenesis and glycerol utilization for gluconeogenesis [42]. *Pparα* was only slightly upregulated in fasted WT but not in homozygotes. This is in line with a study on adult C57BL/6J mice, where a 4-hour fast did not increase *Pparα* expression, but after 16 h 4-fold upregulation was observed [43]. In a study assessing gene expression after 24 and 48 h of fasting in 129/SV

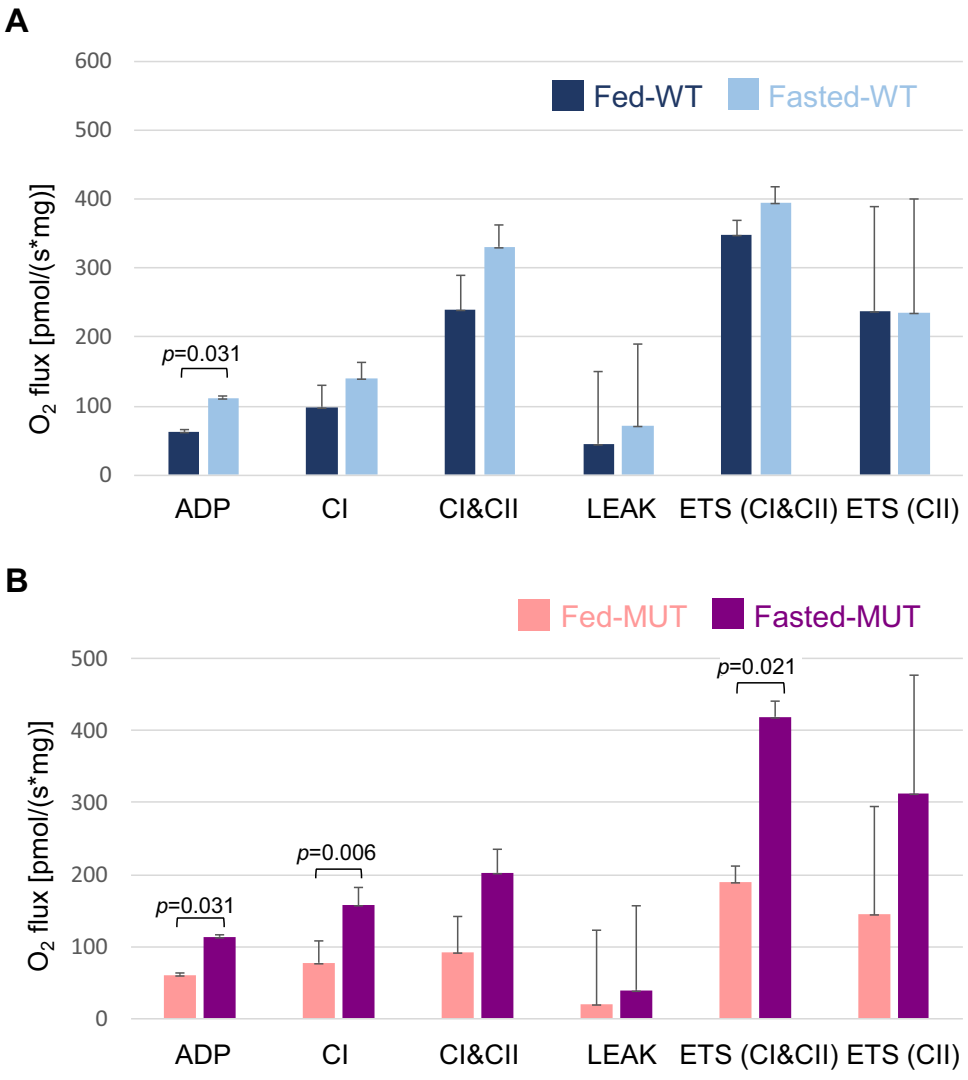

Fig. 4. Effect of fasting on respiration in *Bcs1l*$^{p.S78G}$ liver mitochondria. Oxygen consumption of isolated liver mitochondria from fed or fasted (A) wild-type or (B) mutant mice was determined using an oxygraph. Phosphorylating CI-driven respiration (ADP) was induced by adding malate, pyruvate and ADP. For maximal CI-driven phosphorylating respiration (CI), glutamate was added. Maximal substrate-dependent respiration (CI&CII) was obtained by subsequently adding CII substrate succinate. Basal non-phosphorylating respiration (LEAK) was evaluated with oligomycin. The capacity of the electron transport system (ETS CI&CII and ETS CII) was obtained by titrating with the protonophore FCCP and subsequent inhibition of CI by rotenone. Bars represent means and whiskers SD, significances analyzed with Kruskal-Wallis test.

mice at 8–15 weeks of age, no change in *Pparα* expression was observed [37], whereas in C57BL/6 mice subjected to fasting at P70, the main genes showing increased expressions were *Gdf15*, *Pparα*, *Pgc1α*, *Fgf21*, *Acox1*, *Hmgc2* and *Cpt1α* [39], mainly in line with our findings.

We found very few changes in plasma lipid and lipoprotein levels in fed homozygotes, and also post-heparin LPL and HL activities were similar to those of controls. Only PON1 activity was significantly lower in homozygotes. PON1 is a glycoprotein, mainly synthesized by the liver and circulates bound to HDL particles [44]. It protects LDL from oxidative stress and plays a role in maintaining a low oxidative state in blood circulation [45]. Low PON-1 activity in homozygotes would suggest attenuated anti-oxidant capacity in circulation and thereby attenuated atheroprotection. What is the role of PON-1 regulation in the mutant mice remains to be clarified in more detail in future studies.

Finally, fasting increased mitochondrial respiratory capacity in homozygotes more than in WT. In a study using intermittent (every second day) fasting, increased mitochondrial respiratory capacity was found in liver, but not in brain, heart or skeletal muscle [46]. The mechanism by which fasting increases respiration has not been clarified. Morphologically we noted clear changes in mitochondrial shape and in cristae number and distances, indicating that also the regulation of mitochondrial morphology by 4-hour fasting was preserved despite severe CIII deficiency.

5. Conclusion

The present study shows that systemic lipid mobilization and utilization mechanisms were functional in CIII deficient *Bcs1l* mutant mice, and the mice were able to respond to fasting despite their severe hypoglycemia and chronic energy deficiency. Our results are in line with the current understanding of the pathogenesis of GRACILE syndrome, with liver and kidney being the primary affected organs and the imbalance in systemic energy metabolism and loss of WAT a consequence of these pathologies.

Transparency document

The Transparency document associated this article can be found, in online version.

Declaration of competing interest

The authors declare no competing or financial interest.

Acknowledgements

We acknowledge Janne Purhonen, Folkhälsan Research Center, for valuable technical and intellectual input. We thank M.Sci. Jari Metso for technical assistance and the staff in the BioEM Lab, C-CINA,

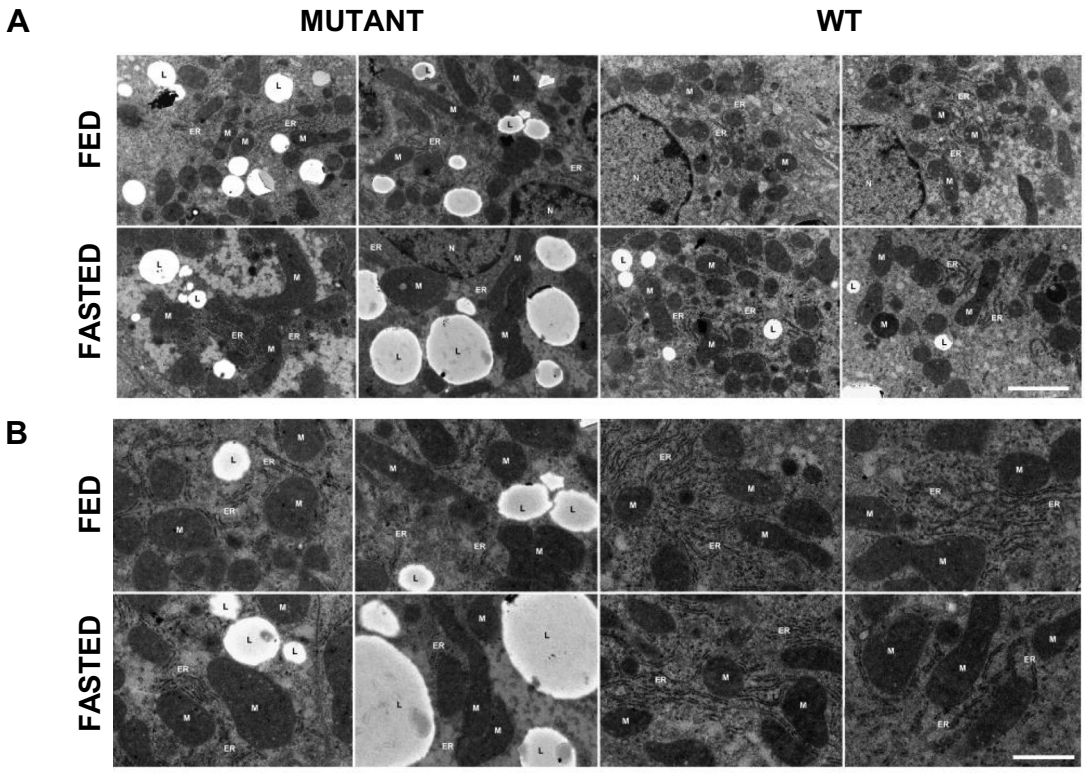

C

	Fed-WT		Fed-MUT		Fasted-WT		Fasted-MUT	
	P26	P27	P26	P27	P26	P27	P26	P27
Elongated shape (%)	2	5	29***	31***	21***	30***	47****	67****
Mean cross-sectional area: roundish (μm²)	2.27	2.28	2.31**	2.37	2.83***	2.97***	2.98***	3.04****
Mean cross-sectional area: elongated (μm²)	4.49	4.76	5.05***	5.39***	5.62***	5.89***	5.98****	6.47****
Crista distance (nm)	37-99	42-112	41-109**	46-197**	48-209***	57-232***	53-218****	66-274****
Crista thickness (nm)	21±2	22±2	22±2**	23±3**	23±2***	23±2***	24±3***	24±2***
No. of cristae per mitochondrion	19±6	18±7	17±7**	14±5**	12±6***	12±8***	10±7****	9±4****

Fig. 5. Effect of fasting on mitochondrial morphology in hepatocytes of *Bcs1l*$^{p.S78G}$ mice. (A) Representative electron micrographs of hepatocytes (M, mitochondria; L, lipid droplets; N, nucleus) and (B) zoom-in to show endoplasmic reticulum (ER) and mitochondria interaction, and (C) quantification of parameters related to mitochondrial morphology at two ages, P26 and P27. The numbers represent data range or mean and standard deviation. Statistics: Mann-Whitney *U* test. $p < 0.05$, $p < 0.01$, $p < 0.001$, $p < 0.0005$ (*, **, *** and **** vs fed WT).

University of Basel, and the Core Facility for Integrated Microscopy (CFIM), Panum Institute, University of Copenhagen, for providing electron microscopy facilities. We thank Cinzia Tiberi (C-CINA) for skillful work and Carola Alampi (C-CINA), Mohamed Chami (C-CINA) and Klaus Qvortrup (CFIM) for practical help with electron microscopy.

Author contribution

HK, VF, NT, JK, MJ conceived and designed the experiments; HK, NT, and EH performed the animal experiments and collected the samples; the laboratory analyses were performed by NT (blood glucose, ketone, lactate), HK, EH, VF (histology), HK, EE (respirometry), MM (TEM), MJ (lipid analyses), HK, EH (qPCR), JK (insulin assay). HK, NT, EAE, EE, MT, MM, JK and VF analyzed the data; NT, IT, RdOF, and MM performed the statistical analyses, NT, EAE, JK, MJ, and VF wrote the manuscript draft; NT, RdOF, VF and JK designed the illustrations; all authors revised the manuscript and have contributed substantially to the work reported.

Financial support

The study was supported by grants from Lund University (VF), the Swedish Research Council (grants 521-2011-3877, 521-2014-3219, VF), the Skåne County Council's Research and Development Foundation (VF, EAE), SUS stiftelser och donationer (VF och EAE) the Kocks foundation (VF), the Erasmus Mundus Programme of the European Union (NT), Jane and Aatos Erkko Foundation (MJ), Academy of Finland (#257545, MJ), and Folkhälsan Research Center (JK, VF).

Appendix A. Supplementary data

Supplementary data to this article can be found online at https://doi.org/10.1016/j.bbadis.2019.165573.

References

[1] A. Garcia-Cazorla, P. de Lonlay, P. Rustin, D. Chretien, G. Touati, D. Rabier, A. Slama, J.M. Saudubray, Mitochondrial respiratory chain deficiencies expressing the enzymatic deficiency in the hepatic tissue: a study of 31 patients, J. Pediatr. 149 (2006) 401–405.
[2] V. Fellman, H. Kotarsky, Mitochondrial hepatopathies in the newborn period, Semin. Fetal Neonatal Med. 16 (2011) 222–228.
[3] E. Fernandez-Vizarra, M. Zeviani, Nuclear gene mutations as the cause of mitochondrial complex III deficiency, Front. Genet. 6 (2015) e134.
[4] C. Nouet, G. Truan, L. Mathieu, G. Dujardin, Functional analysis of yeast bcs1 mutants highlights the role of Bcs1p-specific amino acids in the AAA domain, J. Mol. Biol. 388 (2009) 252–261.
[5] V. Fellman, J. Rapola, H. Pihko, T. Varilo, K.O. Raivio, Iron-overload disease in infants involving fetal growth retardation, lactic acidosis, liver haemosiderosis, and aminoaciduria, Lancet 351 (1998) 490–493.
[6] I. Visapaa, V. Fellman, J. Vesa, A. Dasvarma, J.L. Hutton, V. Kumar, G.S. Payne, M. Makarow, R. van Coster, R.W. Taylor, D.M. Turnbull, A. Suomalainen, L. Peltonen, GRACILE syndrome, a lethal metabolic disorder with iron overload, is caused by a point mutation in BCS1L, Am. J. Hum. Genet. 71 (2002) 863–876.
[7] V. Fellman, S. Lemmela, A. Sajantila, H. Pihko, I. Jarvela, Screening of BCS1L mutations in severe neonatal disorders suspicious for mitochondrial cause, J. Hum. Genet. 53 (2008) 554–558.
[8] P. Leveen, H. Kotarsky, M. Morgelin, R. Karikoski, E. Elmer, V. Fellman, The GRACILE mutation introduced into Bcs1l causes postnatal complex III deficiency: a viable mouse model for mitochondrial hepatopathy, Hepatology 53 (2011) 437–447.
[9] J. Rajendran, N. Tomasic, H. Kotarsky, E. Hansson, V. Velagapudi, J. Kallijarvi, V. Fellman, Effect of high-carbohydrate diet on plasma metabolome in mice with mitochondrial respiratory chain complex III deficiency, Int. J. Mol. Sci. 17 (2016) e1824.
[10] H. Kotarsky, R. Karikoski, M. Morgelin, S. Marjavaara, P. Bergman, D.L. Zhang, J. Smet, R. van Coster, V. Fellman, Characterization of complex III deficiency and liver dysfunction in GRACILE syndrome caused by a BCS1L mutation, Mitochondrion 10 (2010) 497–509.
[11] M. Davoudi, H. Kotarsky, E. Hansson, J. Kallijarvi, V. Fellman, COX7A2L/SCAFI and pre-complex III modify respiratory chain supercomplex formation in different mouse strains with a *Bcs1l* mutation, PLoS One 11 (2016) e0168774.
[12] L.P. Bechmann, R.A. Hannivoort, G. Gerken, G.S. Hotamisligil, M. Trauner, A. Canbay, The interaction of hepatic lipid and glucose metabolism in liver diseases, J. Hepatol. 56 (2012) 952–964.
[13] L. Rui, Energy metabolism in the liver, Compr. Physiol. 4 (2014) 177–197.
[14] J. Lee, J. Choi, S. Scafidi, M.J. Wolfgang, Hepatic fatty acid oxidation restrains systemic catabolism during starvation, Cell Rep. 16 (2016) 201–212.
[15] R.H. Houtkooper, E. Pirinen, J. Auwerx, Sirtuins as regulators of metabolism and healthspan, Nat. Rev. Mol. Cell Biol. 13 (2012) 225–238.
[16] E. Katsyuba, A. Mottis, M. Zietak, F. de Franco, V. van der Velpen, K. Gariani, D. Ryu, L. Cialabrini, O. Matilainen, P. Liscio, N. Giacchè, N. Stokar-Regenscheit, D. Legouis, S. de Seigneux, J. Ivanisevic, N. Raffaelli, K. Schoonjans, R. Pellicciari, J. Auwerx, De novo NAD(+) synthesis enhances mitochondrial function and improves health, Nature 563 (2018) 354–359.
[17] A. Purushotham, T.T. Schug, Q. Xu, S. Surapureddi, X. Guo, X. Li, Hepatocyte-specific deletion of SIRT1 alters fatty acid metabolism and results in hepatic steatosis and inflammation, Cell Metab. 9 (2009) 327–338.
[18] T. Mracek, Z. Drahota, J. Houstek, The function and the role of the mitochondrial glycerol-3-phosphate dehydrogenase in mammalian tissues, Biochim. Biophys. Acta 1827 (2013) 401–410.
[19] M. Adeva-Andany, M. Lopez-Ojen, R. Funcasta-Calderon, E. Ameneiros-Rodriguez, C. Donapetry-Garcia, M. Vila-Altesor, J. Rodriguez-Seijas, Comprehensive review on lactate metabolism in human health, Mitochondrion 17 (2014) 76–100.
[20] H. Schagger, R. de Coo, M.F. Bauer, S. Hofmann, C. Godinot, U. Brandt, Significance of respirasomes for the assembly/stability of human respiratory chain complex I, J. Biol. Chem. 279 (2004) 36349–36353.
[21] N.V. Dudkina, M. Kudryashev, H. Stahlberg, E.J. Boekema, Interaction of complexes I, III, and IV within the bovine respirasome by single particle cryoelectron tomography, Proc. Natl. Acad. Sci. U. S. A. 108 (2011) 15196–15200.
[22] R. Guo, J. Gu, S. Zong, M. Wu, M. Yang, Structure and mechanism of mitochondrial electron transport chain, Biom. J. 41 (2018) 9–20.
[23] G.P. Ables, C.E. Perrone, D. Orentreich, N. Orentreich, Methionine-restricted C57BL/6J mice are resistant to diet-induced obesity and insulin resistance but have low bone density, PLoS One 7 (2012) e51357.
[24] C. Frezza, S. Cipolat, L. Scorrano, Organelle isolation: functional mitochondria from mouse liver, muscle and cultured fibroblasts, Nat. Protoc. 2 (2007) 287–295.
[25] J. Folch, M. Lees, G.H. Sloane Stanley, A simple method for the isolation and purification of total lipides from animal tissues, J. Biol. Chem. 226 (1957) 497–509.
[26] R. van Haperen, A. van Tol, P. Vermeulen, M. Jauhiainen, T. van Gent, P. van den Berg, S. Ehnholm, F. Grosveld, A. van der Kamp, R. de Crom, Human plasma phospholipid transfer protein increases the antiatherogenic potential of high density lipoproteins in transgenic mice, Arterioscler. Thromb. Vasc. Biol. 20 (2000) 1082–1088.
[27] S.E. Heinonen, A.M. Kivela, J. Huusko, M.H. Dijkstra, E. Gurzeler, P.I. Makinen, P. Leppanen, V.M. Olkkonen, U. Eriksson, M. Jauhiainen, S. Yla-Herttuala, The effects of VEGF-A on atherosclerosis, lipoprotein profile, and lipoprotein lipase in hyperlipidaemic mouse models, Cardiovasc. Res. 99 (2013) 716–723.
[28] C. Ehnholm, T. Kuusi, Preparation, characterization, and measurement of hepatic lipase, Methods Enzymol. 129 (1986) 716–738.
[29] M. Jauhiainen, C. Ehnholm, Determination of human plasma phospholipid transfer protein mass and activity, Methods 36 (2005) 97–101.
[30] P. Kleemola, R. Freese, M. Jauhiainen, R. Pahlman, G. Alfthan, M. Mutanen, Dietary determinants of serum paraoxonase activity in healthy humans, Atherosclerosis 160 (2002) 425–432.
[31] D. Pesta, E. Gnaiger, High-resolution respirometry: OXPHOS protocols for human cells and permeabilized fibers from small biopsies of human muscle, Methods Mol. Biol. 810 (2012) 25–58.
[32] S. Cogliati, C. Frezza, M.E. Soriano, T. Varanita, R. Quintana-Cabrera, M. Corrado, S. Cipolat, V. Costa, A. Casarin, L.C. Gomes, E. Perales-Clemente, L. Salviati, P. Fernandez-Silva, J.A. Enriquez, L. Scorrano, Mitochondrial cristae shape determines respiratory chain supercomplexes assembly and respiratory efficiency, Cell 155 (2013) 160–171.
[33] T. Sato, Y. Yoshida, A. Morita, N. Mori, S. Miura, Glycerol-3-phosphate dehydrogenase 1 deficiency induces compensatory amino acid metabolism during fasting in mice, Metabolism 65 (2016) 1646–1656.
[34] J. Purhonen, J. Rajendran, S. Tegelberg, O.P. Smolander, E. Pirinen, J. Kallijärvi, V. Fellman, NAD+ repletion produces no therapeutic effect in mice with respiratory chain complex III deficiency and chronic energy deprivation, FASEB J. (2018), https://doi.org/10.1096/fj.201800090R fj201800090R.
[35] J.M. Ong, T.G. Kirchgessner, M.C. Schotz, P.A. Kern, Insulin increases the synthetic rate and messenger RNA level of lipoprotein lipase in isolated rat adipocytes, J. Biol. Chem. 263 (1988) 12933–12938.
[36] M.Y. Pepino, O. Kuda, D. Samovski, N.A. Abumrad, Structure-function of CD36 and importance of fatty acid signal transduction in fat metabolism, Annu. Rev. Nutr. 34 (2014) 281–303.
[37] M. Bauer, A.C. Hamm, M. Bonaus, A. Jacob, J. Jaekel, H. Schorle, M.J. Pankratz, J.D. Katzenberger, Starvation response in mouse liver shows strong correlation with life-span-prolonging processes, Physiol. Genomics 17 (2004) 230–244.
[38] A. Vila-Brau, A.L. de Sousa-Coelho, J.F. Goncalves, D. Haro, P.F. Marrero, Fsp27/CIDEC is a CREB target gene induced during early fasting in liver and regulated by FA oxidation rate, J. Lipid Res. 54 (2013) 592–601.
[39] M. Zhang, W. Sun, J. Qian, Y. Tang, Fasting exacerbates hepatic growth differentiation factor 15 to promote fatty acid beta-oxidation and ketogenesis via activating XBP1 signaling in liver, Redox Biol. 16 (2018) 87–96.
[40] J. Purhonen, J. Rajendran, M. Morgelin, K. Uusi-Rauva, S. Katayama, K. Krjutskov, E. Einarsdottir, V. Velagapudi, J. Kere, M. Jauhiainen, V. Fellman, J. Kallijärvi, Ketogenic diet attenuates hepatopathy in mouse model of respiratory chain complex III deficiency caused by a *Bcs1l* mutation, Sci. Rep. 7 (2017) e957.
[41] H. Kotarsky, M. Keller, M. Davoudi, P. Leveen, R. Karikoski, D.P. Enot, V. Fellman, Metabolite profiles reveal energy failure and impaired beta-oxidation in liver of

mice with complex III deficiency due to a BCS1L mutation, PLoS One 7 (2012) e41156.
[42] D.G. Cotter, B. Ercal, D.A. d'Avignon, D.J. Dietzen, P.A. Crawford, Impairments of hepatic gluconeogenesis and ketogenesis in PPARalpha-deficient neonatal mice, Am. J. Physiol. Endocrinol. Metab. 307 (2014) e176–e185.
[43] C.E. Geisler, C. Hepler, M.R. Higgins, B.J. Renquist, Hepatic adaptations to maintain metabolic homeostasis in response to fasting and refeeding in mice, Nutr. Metab. (Lond.) 13 (2016) 62 e1-13.
[44] B.N. La Du, Structural and functional diversity of paraoxonases, Nat. Med. 2 (1996) 1186–1187.
[45] L.P. Precourt, D. Amre, M.C. Denis, J.C. Lavoie, E. Delvin, E. Seidman, E. Levy, The three-gene paraoxonase family: physiologic roles, actions and regulation, Atherosclerosis 214 (2011) 20–36.
[46] B. Chausse, M.A. Vieira-Lara, A.B. Sanchez, M.H. Medeiros, A.J. Kowaltowski, Intermittent fasting results in tissue-specific changes in bioenergetics and redox state, PLoS One 10 (2015) e0120413.